Journal of Fluorescence
https://doi.org/10.1007/s10895-019-02351-x

ORIGINAL ARTICLE

A Highly Selective "Turn-on" Fluorescent Probe for Detection of Fe^{3+} in Cells

Xiaorui Cao[1] · Feifei Zhang[1] · Yinjuan Bai[1] · Xiaohu Ding[1] · Wei Sun

Received: 28 November 2018 / Accepted: 14 January 2019

Abstract

A new "turn-on" fluorescent probe **Py** based on rhodamine and piperonaldehyde was designed and synthesized for detecting Fe^{3+} in cells. The free probe **Py** was non-fluorescent. While only upon addition of Fe^{3+}, the significant increase of the fluorescence and color were observed which could be visible directly by "naked-eye". The probe **Py** shows high selectivity and sensitivity for Fe^{3+} over other common metal ions in EtOH-H_2O (3/2, *v*/v) mixed solution. The association constant and the detection limit were calculated to be $4.81 \times 10^4\ M^{-1}$ and 1.18×10^{-8} mol/L respectively. The introduction of piperonaldehyde unit could increase probe rigidity which could enhance its optical properties. Meanwhile, the binding mode between **Py** and Fe^{3+} was found to be a 1:1 complex formation. The density functional theory (DFT) calculations were performed which would further confirm the recognition mechanism between probe **Py** and Fe^{3+}. In addition, the probe has been proved to be reversible for detecting Fe^{3+}. Moreover, the probe **Py** was used to detect Fe^{3+} in cells successfully.

Keywords Fluorescent probe · Rhodamine · Fe^{3+} · Cell imaging · DFT calculations

Introduction

The normal life activities of the human body are inseparable from trace elements. Iron as one of the most essential trace elements, it exists in ferrous (Fe^{2+}) and ferric (Fe^{3+}) forms in living organism. The iron ions play an important role in the fundamental physiological processes of living systems. It is related to the biological cellular metabolism, gene transcription, oxygen metabolism, electron transit, protein synthesis, enzyme catalysis, DNA and RNA synthesis and so on [1–4]. Whether the iron ion content in the organism is excessive or deficient will induce various diseases such as heart failure, neurodegenerative, anemia, liver and kidney damage and diabetes [5–8]. No that Fe^{2+} can be easily converted to Fe^{3+}, discrimination of Fe^{3+} from Fe^{2+} is important to understand the biological processes such as iron metabolism. So it is very important to design a good method which could detect Fe^{3+} in biological organism. Over the past years, many fluorescent sensors for Fe^{3+} have been reported because of its simple operation, high sensitivity, selectivity and response speed, as well as low detection limit [9, 10]. In the early days, most of them are "turn-off" types, because of the paramagnetic nature of Fe^{3+} which could quench the fluorescence of probe [11, 12]. Now many "turn-on" fluorescent sensors based on Rhodamine family derivatives have been reported due to their long absorption and emission wavelengths, high fluorescence quantum yield, large absorption coefficient and the property of spirocyclic closed ring (non-fluorescent and colorless) and ring-opened (fluorescent and strong absorption) of the rhodamine family compounds which could efficiently respond to metal ions [13–25]. A solvent-dependent fluorescent probe based on rhodamine B derivative has been reported because of its high selectivity and low detection limit [26]. A optical–electrochemical multichannel chemosensor has been reported which could detect Fe^{3+} through multiple physical responses [27]. A reversible probe based on Rhodamine B also has been reported but it does not show the reversibility well [28]. A fluorescent probe based on rhodamine6G for detecting Fe^{3+}

Electronic supplementary material The online version of this article (https://doi.org/10.1007/s10895-019-02351-x) contains supplementary material, which is available to authorized users.

✉ Yinjuan Bai
baiyinjuan@nwu.edu.cn

[1] Key Laboratory of Synthetic and Natural Functional Molecule Chemistry of Ministry of Education, College of Chemistry and Materials Science, Northwest University, Xi'an, Shaanxi 710127, People's Republic of China

Published online: 06 February 2019

in water has been reported, but it is hard to distinguish Fe^{3+} from Hg^{2+},Cr^{3+} directly in water [29]. Furthermore, there are still some deficiencies for most probes, such as very poor solubility in water [30] and interfered a little to other ions such as Cr^{3+}, Cu^{2+} [31, 32]. Other than this, some probes are cell impermeable or need long response time [33]. In addition, strict working condition and high excited energy could limit the biological applications of them [34, 35]. What's more, only a few probes having been reported are reversible due to their reaction-based nature [36]. Therefore, designing a reversible and highly selective probe with better biological properties is still full of challenges.

In this work, we synthesized a fluorescent probe **Py** (Scheme 1) based on rhodamine and piperonaldehyde, which was characterized by IR, NMR and HRMS. The introduction of piperonaldehyde unit could increase the rigidity of the probe which could enhance its optical performance. In addition, the imide structure can coordinate well with metal ions. The probe **Py** exhibits high selectivity and sensitivity for Fe^{3+} detection in EtOH-H_2O (3/2, *v*/v) over other commonly coexistent metal ions. In addition, the probe **Py** can be used as a "naked-eye" sensor to detect Fe^{3+} by significant color change. The limit of probe **Py** detection for Fe^{3+} was found to be as low as 1.18×10^{-8} mol/L which was lower than most researches [36]. The DFT calculations further better explained the recognition mechanism between probe **Py** and Fe^{3+}. We also confirmed the reversibility of the probe for detection Fe^{3+} which can reduce the cost of its application. The most important is that the biological imaging of the probe **Py** was used in SGC7901 cells successfully and had been tested to have low biological toxicity.

Experimental

General Information

Mass spectra was performed with Bruckermicro TOF-QII.^{1}H and ^{13}C NMR spectra were recorded on a Varian unity INOVA-400 MHz spectrometer, using the solvent the TMS signal as an internal standard. The fluorescence spectra were measured on HITACHI F-4500 fluorescence spectrophotometer.IR spectra were taken on a Brucker EQUIOX-55 spectrometer with KBr pellets. The absorbance spectra were recorded on a Shimadzu UV-1700 spectrophotometer. Melting points were obtained on a Laboratory Devices XT4B melting apparatus and uncorrected. All the solvents and reagents (analytical grade) were purchased from commercial suppliers and used without further purification. Double distilled water was used throughout the experiment. The solutions of metal ions were prepared from corresponding nitrate and chloride salts.

Fluorescence quantum yield (φ_f) is the ratio of the number of photons emitted after absorption of energy by the fluorescent material to the number of photons absorbed. In this paper, 0.05 mol/L rhodamine B solution is used as reference solution, and then we calculated the fluorescence quantum yield of the sample under test[Eq. (1)] [37]:

$$\varphi_f = \varphi_s \times \frac{(F_f \times A_s)}{(F_s \times A_f)}$$

φ_f and φ_s in the formula are the fluorescence quantum yield of the sample to be measured and the reference sample, respectively; A_f and A_s are the absorbance of the excitation light

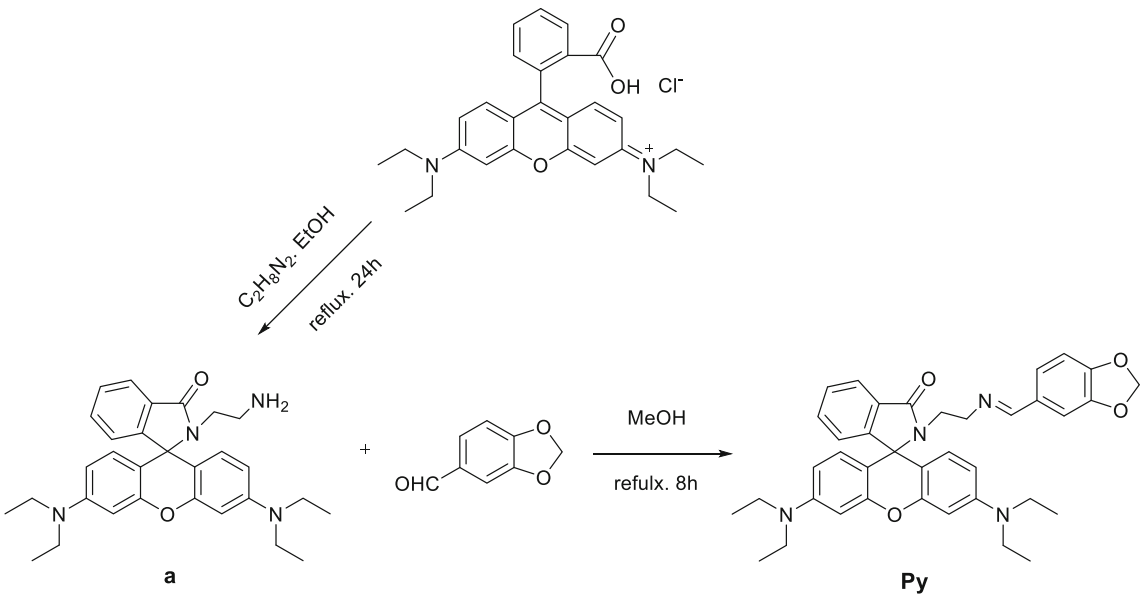

Scheme 1 The synthetic route to **Py**

of the sample and the reference sample respectively. The fluorescence quantum yield of the compound **Py** was measured to be 0.31 (At the same excitation wavelength and in the same solvent).

Preparation of the Test Solution

A stock solution of probe **Py** (2×10^{-4} mol/L): in a 25 mL volumetric flask, 154.1 mg of **Py** was dissolved in dichloromethane and then diluted to the mark with ethanol. 0.5 mL of the solution was then transferred to a 25 mL volumetric flask and diluted to the mark with ethanol.

Stock solutions of the metal ions were prepared in double distilled water with the metal salts (KCl, NaCl, LiCl, $MgCl_2$, $BaCl_2$, $AgNO_3$, $CaCl_2$, $ZnCl_2$, $CdCl_2$, $Cu(NO_3)_2$, $MnCl_2$, $CoCl_2$, $NiCl_2$, $PbCl_2$, $Al(NO_3)_3$, $FeCl_3$, $HgCl_2$, $CrCl_3$,$FeCl_2$).

Syntheses

Rhodamine B ethylenediamide (a) was synthesized from rhodamine B and ethylenediamine used the literature procedure [38]. yield 73.6%. ESI-HRMS Calcd for ($C_{30}H_{36}N_4O_2$+ H^+) m/z = 485.2916. Found: 485.2623 ($M + H^+$).

Synthesis of probe **Py**: In a single necked round-bottomed flask, compound a (0.49 g, 1 mmol) and pepper aldehyde (0.18 g, 1 mmol) were mixed into 20 mL methanol solution. The mixture was heated to reflux. The process of reaction was monitored by TLC. After cooled to room temperature, the precipitate was separated by filtration and further purified by recrystallizing from ethanol to obtained pink solid product. Yield 53.5%, m.p.183–184 °C. IR (KBr) ν_{max}/cm^{-1}: 3432, 3376, 3085, 3043, 2973, 2896, 1697, 1617, 1550, 1517, 1448, 1376, 1349, 1299, 1249, 1228, 1118, 1039, 929, 813, 752, 698, 601, 536.^{1}H NMR (400 MHz; $CDCl_3$;Me_4Si), δ (ppm): 7.93 (s, 1H, Ar*H*), 7.91–7.89 (m, 1H,Ar*H*), 7.42–7.40 (m, 2H, Ar*H*), 7.20 (d, J = 1.5 Hz, 1H,Ar*H*), 7.07–7.05 (m, 1H, Ar*H*), 6.99 (dd, J_1 = 8.0, J_2 = 1.5 Hz, 1H, Ar*H*), 6.75 (d, J = 8.0 Hz, 1H,Ar*H*), 6.44 (d, J = 8.8 Hz, 2H, Ar*H*), 6.38 (d, J = 2.6 Hz, 2H, Ar*H*), 6.25 (dd, J_1 = 6.4, J_2 = 2.6 Hz, 2H, Ar*H*), 5.95 (s, 2H, OCH_2O), 3.41 (s, 4H, NCH_2CH_2N), 3.32 (q, J = 7.1 Hz, 8H, $N(CH_2CH_3)_4$), 1.16 (t, J = 7.0 Hz, 12H, $N(CH_2CH_3)_4$). ^{13}C NMR (101 MHz, $CDCl_3$), δ (ppm): 168.6, 161.9, 154.1, 153.5, 149.7, 149.05, 147.8, 132.1, 131.1, 129.2, 128.2, 124.4, 123.7, 122.7, 106.8, 105.6, 101.2, 97.9, 64.96, 58.9, 44.3, 41.3, 12.7. ESI-HRMS calcd for ($C_{38}H_{40}N_4O_4 + H^+$) m/z = 617.3128. Found: 617.3125 ($M + H^+$).

Cells Imaging Study

The probe was dissolved in a small amount of DMSO and then dissolved it in water to form a stock solution. The cell lines were then added with **Py** (in aqueous DMSO, culture medium) to obtain a final concentration of 10 μM **Py** and incubated under reoxygenation (95% air, 5% CO_2) for 30 min at 37 °C. After the incubation, the cell lines were washed with PBS to remove excess probe and monitored with confocal microscope. Finally, these cells were treated with Fe^{3+} ion solution (10 μM) and fresh DMEM culture medium for 1 h at 37 °C and then washed with PBS for three times. Cells were observed using confocal fluorescence microscopy at $\lambda_{ex}/\lambda_{em}$ = 550 nm/560–680 nm.

Cells Toxicity Study

Cells toxicity and survival rate study were tested by CCK-8 assay. Cells were seeded into 96-well plates and cultured at 37 °C (5% CO_2) for 24 h, different concentrations of probe **Py** (0, 6.25, 12.5, 25, 50 and 100 μM) were then added to the wells. After incubation for 24 h, CCK-8 (10% in culture medium) was added to each well, and the plate was incubated for another 1 h. Absorbance was measured at 450 nm. All experiments were repeated three times, and the data were presented as the percentage of control cells.

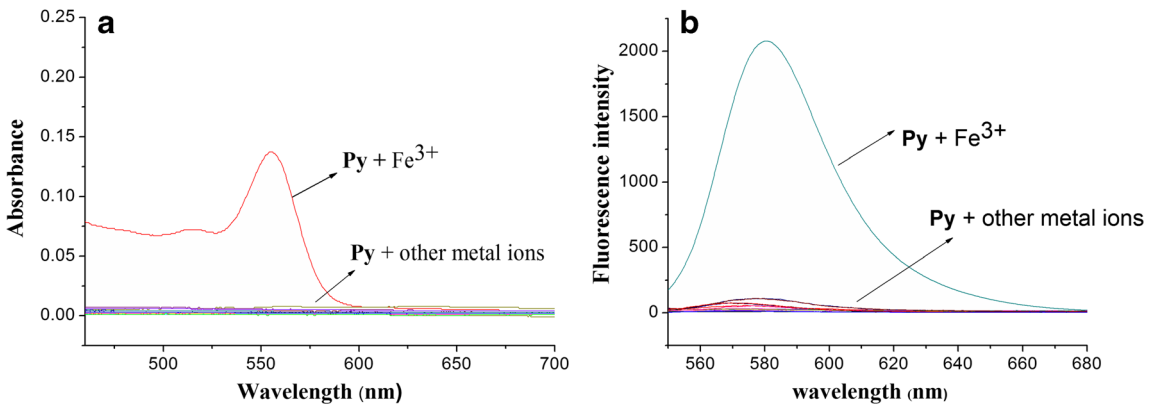

Fig. 1 **a** The UV-vis spectra of **Py** solution in the presence of several different metal ions. **b** Fluorescence spectra of **Py** (20 μM) in the presence of several different metal ions (20 μM) in EtOH-H_2O (3/2, *v*/v) solution, λ_{ex} = 550 nm

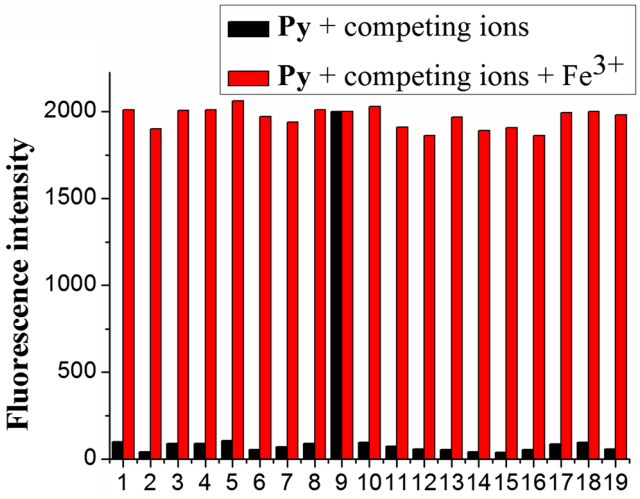

Fig. 2 Fluorescence intensity changes of **Py** (20 μM) upon the addition of various metal ions (20 μM) in the absence and presence of Fe^{3+} (20 μM) in EtOH-H_2O (3/2, *v*/v) solution. 1 Ag^{+}, 2 Al^{3+}, 3 Ba^{2+}, 4 Ca^{2+}, 5 Cd^{2+}, 6 Co^{2+}, 7 Cr^{3+}, 8 Cu^{2+}, 9 Fe^{3+}, 10 Hg^{2+}, 11 K^{+}, 12 Li^{+}, 13 Mg^{2+}, 14 Mn^{2+}, 15 Na^{+}, 16 Ni^{2+}, 17 Pd^{2+}, 18 Zn^{2+},19 Fe^{2+} (λ_{ex} = 550 nm/λ_{em} = 580 nm)

Results and Discussion

Synthesis of Probe Py

The synthesis of **Py** was shown in Scheme 1. It was characterized by ^{1}H NMR, ^{13}C NMR, IR and HRMS, the corresponding spectra were shown in the Supporting Information**.**

Selective Study

The UV–vis absorption and fluorescence spectral behavior of **Py** to a series of metal ions were investigated, including Ag^{+}, Al^{3+}, Ba^{2+}, Ca^{2+}, Cd^{2+}, Co^{2+}, Cr^{3+}, Cu^{2+}, Fe^{3+}, Hg^{2+}, K^{+}, Li^{+}, Mg^{2+}, Mn^{2+}, Na^{+}, Ni^{2+}, Pd^{2+}, $Zn^{2+}$and Fe^{2+} respectively. As shown in Fig. 1a, a remarkable enhancement in absorption spectra at 550 nm was observed when Fe^{3+} was added while all other metal ions did not make apparent absorbance enhancement. Moreover, upon the addition of Fe^{3+}, the solution of probe **Py** immediately yield a pink color **(Fig. S1)**. Under the identical condition, no obvious response could be observed with the addition of other metal ions. As shown in Fig. 1b, the same results in fluorescence spectra were observed at 580 nm. When added other metal ions, the probe **Py** would not combine these ions, so it keep five-membered spirolactam structure. However, when Fe^{3+} was added, the probe **Py** lactam ring was opened, resulting in strong fluorescence and color changes. These results demonstrated that probe **Py** had a high selectivity for Fe^{3+} over other ions and it could serve as a fluorescent and"naked eye"probe for detecting Fe^{3+} in EtOH-H_2O mixture.

Interference Study

Besides Fe^{3+}, there are many other metal ions in the living body. Therefore, in order to further test the selectivity of **Py** to Fe^{3+} from other ions, the selectivity of **Py** (20 μM) for Fe^{3+} over other metal ions (1.0 equiv) were explored by the competition assay in the presence of other various metal ions. As shown in Fig. 2, there was almost no effect on the fluorescence of Fe^{3+}-**Py** in the presence of various interference metal ions. Selectivity and competition experiments indicated that probe **Py** could specifically detect Fe^{3+} with little interference from other commonly coexistent ions.

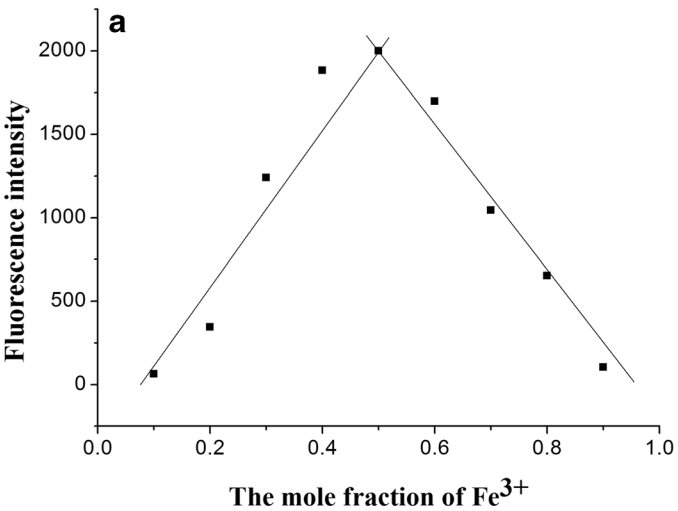

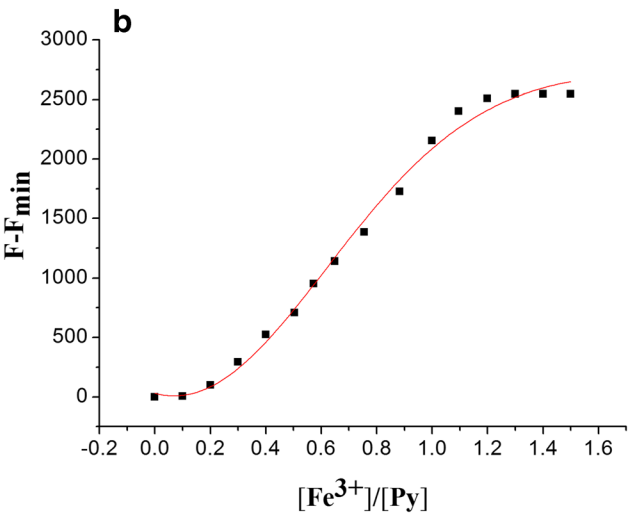

Fig. 3 **a** The Job's plot of probe **Py** and Fe^{3+} (the total concentration was 40 μM) in EtOH-H_2O (3/2, *v*/v) solution; (**b**) None-linear plot of probe **Py** (20 μM) assuming a 1:1 stoichiometry for association between probe **Py** and Fe^{3+} in Ethanol/H_2O (v/v, 3/2) solution by fluorescence spectroscopy. λ_{em} = 550 nm/λ_{em} = 580 nm

Scheme 2 The binding mechanism between **Py** and Fe^{3+}

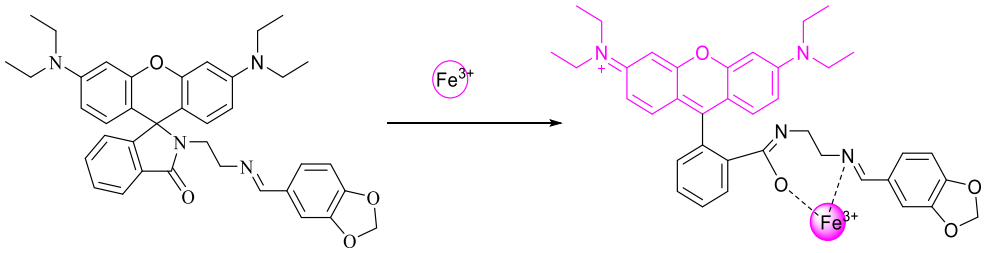

Effect of Fe^{3+} Concentration Study

Fluorescence and UV-vis titration experiments were also carried out. Under neutral conditions, rhodamine-type probes exist in a spiro ring structure which makes **Py** colorless and non-fluorescent. The intensity of fluorescence at 580 nm and UV absorption at 550 nm are increasing with the the concentration of Fe^{3+} (0–1.25 equiv) increased (**Fig. S2** and **S3**). It is attributed to the delocalization effects in the xanthene moiety of the rhodamine. These results clearly indicated that Fe^{3+} could bind to the probe **Py**, thus the probe **Py** lactam ring was opened and formed a highly delocalized p-π conjugated structure. Therefore, significant enhancement of absorbance and fluorescence were observed.

According to the Job's plots, the fluorescence intensity reached maximum when the molar fraction of Fe^{3+} was 0.5 (Fig. 3a). This showed that the binding stoichiometry of Fe^{3+} to the probe **Py** molecule was found to be 1:1. Conceivably, Fe^{3+} with probe **Py** formed a 1:1 metal complex which induced the spirane structure of probe **Py** to be opened. The binding model was proposed and shown in Scheme 2.

The fluorescence spectrum association constants of Fe^{3+} were calculated by nonlinear fitting (Fig. 3b) using the following formula[Eq. (2)] [39]:

$$\Delta F = \frac{\Delta\beta\left([H]_0 + [G]_0 + {}^1/_{K_a}\right) \pm \sqrt{\Delta\beta^2\left([H]_0 + [G]_0 + {}^1/_{K_a}\right)^2 - 4\Delta\beta^2[H]_0[G]_0}}{2}$$

ΔF is the change in the fluorescence intensity of the **Py** upon gradual addition of the Fe^{3+}, and Δβ refers to the different constant of the free host and the interaction complex. The total concentrations of host and guest are denoted by $[H]_0$ and $[G]_0$, respectively. The association constant of **Py** with Fe^{3+} was accordingly calculated to be 4.81×10^4 M^{-1} (R = 0.9935). The limit of detection for Fe^{3+} was calculated to be 1.18×10^{-8} mol/L. These results indicated that probe **Py** holds great potential for using in the development of sensor materials for Fe^{3+}.

Effect of pH and Response Time Study

Normally, the spironolactone ring of the rhodamine derivatives would be opened in acidic media. Therefore, it is necessary to evaluate the effect of pH on the fluorescence of probe **Py**. The effects of pH on probe **Py** experiment was evaluated in the different pH media (Fig. 4a). No obvious enhancement of fluorescence at 580 nm was observed in the pH range of 5.0–12.0, suggesting that it is insusceptible to the change of acid–base solution. However, in the presence of Fe^{3+}, a remarkable fluorescence emission band at 580 nm was formed under different pH conditions. It showed that the pH corresponded to the highest response approximately in 4.0–8.0, which revealed that the probe **Py** for Fe^{3+} could work well in approximate physiological conditions and with very low background response. When the pH exceed 10.0, the fluorescence of probe **Py** would vanish, this is because the high concentration of OH^- would combine with Fe^{3+} to form $Fe(OH)_3$. As shown in Fig. 4b, with the increase of the reaction time, the fluorescence intensity of probe **Py** with Fe^{3+} increased and reached equilibrium within 10 min. These indicated that probe **Py** could serve as an efficient probe for detection of Fe^{3+} in a neutral medium in a short time.

Cell Imaging and Cytotoxicity Study

To test the potential biological application of probe **Py** for detecting Fe^{3+} in living cells, the fluorescence imaging was recorded using confocal fluorescence microscopy. The human cancer cells SGC7901 (stomach cells) were cultured in high glucose type DMEM culture medium and then further incubated with the probe **Py** under reoxygenation (95% air, 5% CO_2) for 30 min at 37 °C. After incubation, excess unbound probe were washed with PBS buffer. No intracellular fluorescence was observed inside the cells (Fig. 5a) but the bright field image of cells was seen clearly in Fig. 5b which proved that the cell could remain in good condition after incubated with probe. These cells were treated with Fe^{3+} (10 μM) for 1 h at 37 °C and then washed with PBS buffer to remove excess

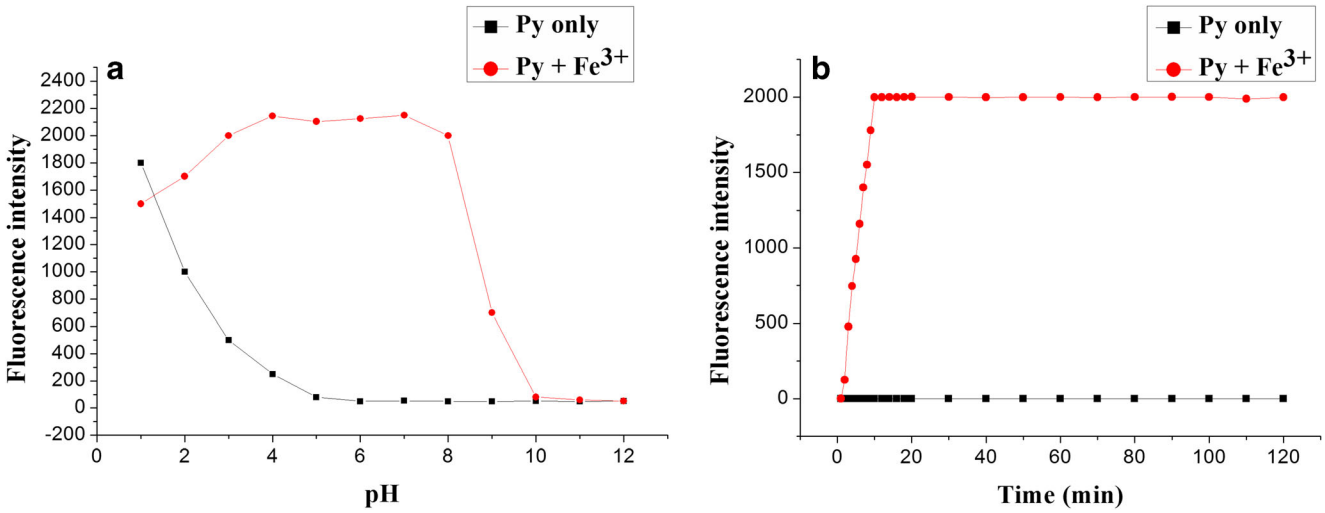

Fig. 4 **a** Effect of pH on the fluorescence intensity of **Py** (black line) and **Py**-Fe^{3+} (red line). **b** Effect of time on the fluorescence intensity of **Py** (black line) and **Py**-Fe^{3+} (red line), $\lambda_{ex} = 550$ nm/$\lambda_{em} = 580$ nm

Fe^{3+}. Obviously, a significant fluorescence from the intracellular area was observed (Fig. 5c), this indicated that probe **Py** has the fine cell membrane permeability and could be used to detect Fe^{3+} in cells. The overlay image (Fig. 5d) of bright field and fluorescence image further confirmed that the fluorescent signals were localized in cells. As shown in **Table S1** (Supporting Information), the cells survival rate was as high as 82.43% after they were incubated with 100 μM probe **Py** for 24 h. These datas demonstrated that probe **Py** has superior biocompatibility and low cytotoxicity. Therefore it has the potential value for detecting Fe^{3+} in the biological system due to its ideal chemical, biological and spectroscopic properties.

Theoretical Calculations

In order to better understand the reaction mechanism between probe **Py** and Fe^{3+}, the DFT calculations of **Py** and **Py**-Fe^{3+} complex were performed and the basis set was B3LYP/6-31G** [23, 40, 41]. The optimized geometries of **Py** and **Py**-Fe^{3+} complex were shown in **Fig. S4**. As shown in **Fig. S4b**, the binding sites with Fe^{3+} are N and O atoms. According to NBO analysis [40] of the lone pair orbitals of N and O atoms in the probe **Py**, the Fukui function of O (0.036), N_2 (0.014), and N_1 (−0.007) were calculated respectively. The f value of the N_2 and O atoms were shown to be larger than that of the N_1 atom. These indicated that the O and

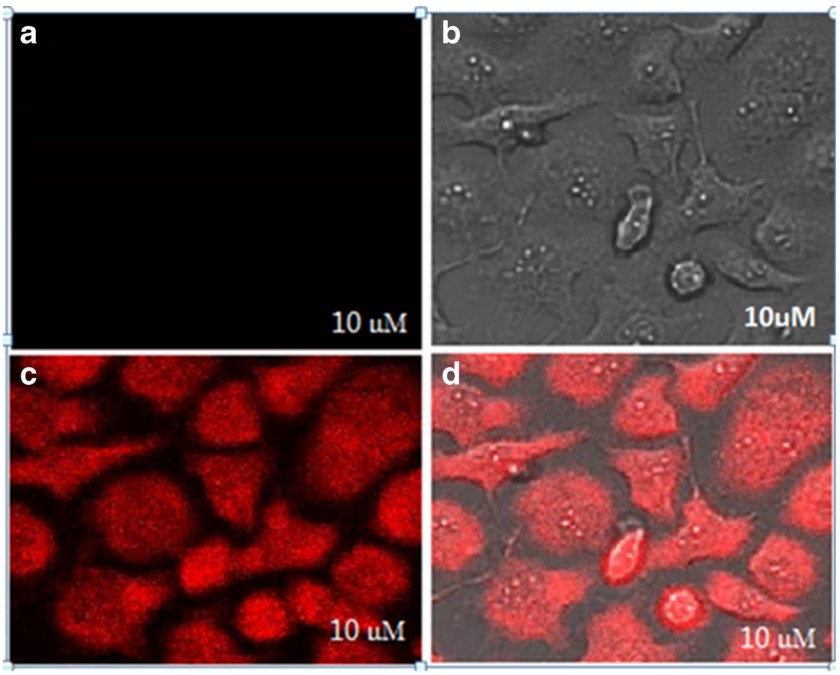

Fig. 5 Confocal dark-field fluorescence image of SGC7901 cells incubated with **Py** (10 μM) for 30 min. **a** Dark-field image (**b**) Bright-field image. **c** Fluorescence image of the cells in (**b**) further incubated with Fe^{3+} (10 μM) for 1.0 h. **d** Overlay image of (**b**) and (**c**)

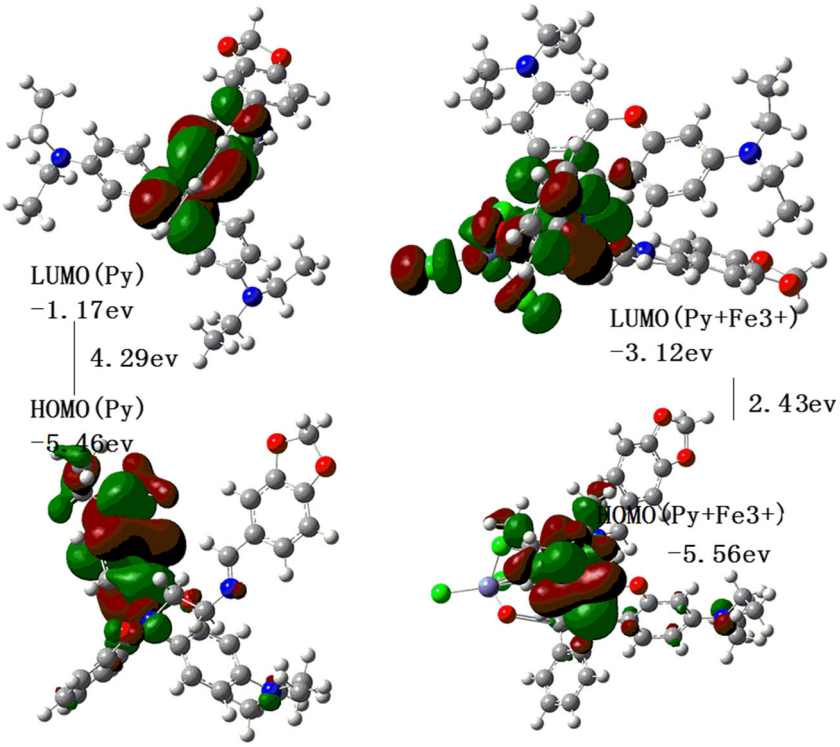

Fig. 6 HOMO and LUMO orbitals of probe **Py** and the **Py**-Fe^{3+}complex

N_2 are better active sites than N_1 atom which facilitates its contact with Fe^{3+}. Therefore, compared with the N_1 atom, the combination of the Fe^{3+} with the N_2 and O atoms should be more energetically favorable. As shown in Scheme 2, the spirocyclic form of probe **Py** was opened by the transfer of electrons, which induce the changes in fluorescence. In summary, Fe^{3+} is more likely to complex with N_2 and O atom than N_1, thus a 1:1 Py-Fe3+ complex was formed. We also calculated HOMO and LUMO orbitals of probe **Py** and the **Py**-Fe^{3+} complex. As shown in Fig. 6, in probe **Py**, the HOMO are spread out on the xanthenes of the rhodamineB moiety while the LUMO are centered on the spirocycle of the rhodamineB moiety. In **Py**-Fe^{3+} complex, maximum electron concentrated on the rhodamineB moiety at HOMO, while the major electron distribution was on metal centre at LUMO. The energy gap (ΔE) exhibited that the binding of Fe^{3+} to **Py** lowered the HOMO-LUMO energy gap of the complex and stabilized the system. In **Py**-Fe^{3+} complex, the distance of Fe^{3+} to O and N_2 are calculated to be 2.02 and 1.95 A respectively, while it is 2.63 A in "Fe^{3+}-N_1" bond. These results further explained the model of reaction mechanism between probe **Py** and Fe^{3+}.

Reversibility Study

To further study the reversibility of the probe **Py** for detecting Fe^{3+}, we added ethylenediamine (ED) (20 μM) to the solution of **Py**-Fe^{3+} (20 μM), as show in Fig. 7, the fluorescence intensity changed to weak (A → B). When Fe^{3+} (20 μM) were added to the system again, however, the fluorescence intensity enhanced again (B → C). The above process can be repeated several cycles and still remained the same orderliness without significant changes in the fluorescence spectrum. This proved that the probe detects Fe^{3+} is reversible and can be reused.

Comparison with Other Probes

We also compared the probe **Py** with some other previously reported Fe^{3+} fluorescent probes. As shown in Table 1, most

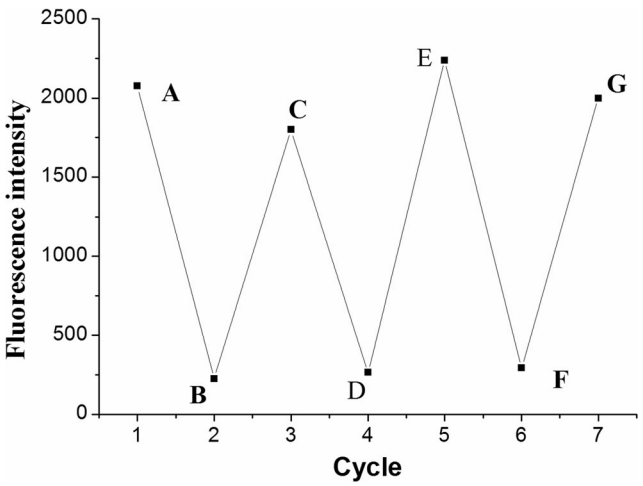

Fig. 7 The fluorescence intensity for cycles of the recognition process of **Py** (20 μM) toward Fe^{3+} (**2**0 μM) in EtOH-H2O (3/2, *v*/v) solution, λ_{ex} = 550 nm/λ_{em} = 580 nm

Table 1 The comparison of **Py** with some other rhodamine derivative probes for Fe^{3+}.

Sensor	Solution (V/V)	LOD (μM)	Interference	Reference
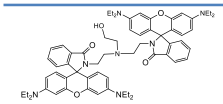	MeOH/H2O = 1:1,	0.107	Al^{3+},Cr^{3+}	[4]
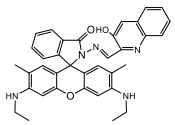	aqueous medium	0.033	Fe^{2+}	[32]
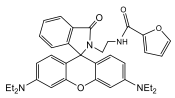	MeOH/H2O = 1:1,	0.437	Al^{3+},Cu^{2+}	[33]
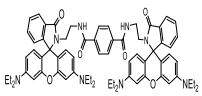	THF-H2O = 4/6,	0.0231	Al^{3+},Hg^{2+}	[36]
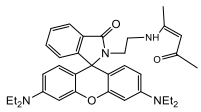	Water (PH = 5.5)	1.0	Cu^{2+}	[42]
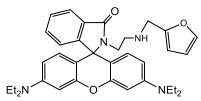	EtOH/H2O = 1:1	0.025	Al^{3+}	[43]
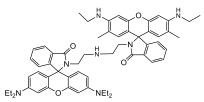	EtOH/H2O = 1:1	0.16	Fe^{2+},Hg^{2+}	[44]
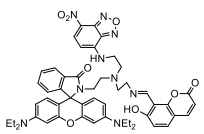	CH3CN/H2O = (97/3)	0.074		[25]
Py	EtOH/H2O = 3:2	0.0118		This work

of them are not only interfered to other metal ions but also have higher detection limit. However, probe **Py** shows higher selectivity and lower detection limit than most of them. Therefore, it has some certain advantages in application.

Conclusion

In summary, we synthesized a highly selective "turn-on" fluorescent probe **Py** for detecting Fe^{3+}. In addition, it can be

recognized by the "naked eye". The probe **Py** shows high selectivity, sensitivity, reversibility and low cytotoxicity. The reaction mechanism between probe **Py** and Fe^{3+} were performed using DFT calculation. Importantly, the probe **Py** was used to sense Fe^{3+} in cells successfully. These features will make it more potential for biological applications.

Acknowledgements We gratefully acknowledge financial support from the National Natural Science Foundation of China (Grant no.21042002).

References

1. Zhang Y, Wang Y-T, Kang X-X, Ge M, Feng H-Y, Han J, Wang D-H, Zhao D-Z (2018) Azobenzene disperse dye-based colorimetric probe for naked eye detection of Cu^{2+} in aqueous media: spectral properties, theoretical insights, and applications. J Photoch Photobio A 356:652–660
2. Ozdemir M, Zhang Y, Guo M (2018) A highly selective "off-on" fluorescent sensor for subcellular visualization of labile iron(III) in living cells. Inorg Chem Commun 90:73–77
3. Wang J, Zhang D, Liu Y, Ding P, Wang C, Ye Y, Zhao Y (2014) A N-stablization rhodamine-based fluorescent chemosensor for Fe^{3+} in aqueous solution and its application in bioimaging. Sensors Actuators B Chem 191:344–350
4. Zhu C, Wang M, Qiu L, Hao S, Li K, Guo Z, He W (2018) A mitochondria-targeting fluorescent Fe^{3+} probe and its application in labile Fe^{3+} monitoring via imaging and flow cytometry. Dyes Pigments 157:328–333
5. Yang Z, Bai X, Ma S, Liu X, Zhao S, Yang Z (2017) A benzoxazole functionalized fluorescent probe for selective Fe^{3+} detection and intracellular imaging in living cells. Anal Methods 9:18–22
6. Sen S, Sarkar S, Chattopadhyay B, Moirangthem A, Basu A, Dhara K, Chattopadhyay P (2012) A ratiometric fluorescent chemosensor for iron: discrimination of Fe^{2+} and Fe^{3+} and living cell application. Analyst 137:3335–3342
7. Long L, Zhou L, Lin W, Meng S, Gong A, Chi Z (2014) A ratiometric fluorescent probe for iron(III) and its application for detection of iron(III) in human blood serum. Anal Chim Acta 812:145–151
8. Bao X, Shi J, Nie X, Zhou B, Wang X, Zhang L, Liao H, Pang T (2014) A new rhodamine B-based 'on-off' chemical sensor with high selectivity and sensitivity toward Fe(3+) and its imaging in living cells. Bioorg Med Chem 22:4826–4835
9. Jeong Y, Yoon J (2012) Recent progress on fluorescent chemosensors for metal ions. Inorg Chim Acta 381:2–14
10. Xu H, Ding H, Li G, Fan C, Liu G, Pu S (2017) A highly selective fluorescent chemosensor for Fe^{3+} based on a new diarylethene with a rhodamine 6G unit. RSC Adv 7:29827–29834
11. Yang Y, Wang X, Cui Q, Cao Q, Li L (2016) Self-assembly of fluorescent organic nanoparticles for Iron(III) sensing and cellular imaging. ACS Appl Mater Interfaces 8:7440–7448
12. Zheng M, Tan H, Xie Z, Zhang L, Jing X, Sun Z (2013) Fast response and high sensitivity europium metal organic framework fluorescent probe with chelating Terpyridine sites for Fe^{3+}. ACS Appl Mater Interfaces 5:1078–1083
13. Pires MM, Chmielewski J (2008) Fluorescence imaging of cellular glutathione using a latent rhodamine. Org Lett 10:837–840
14. Zhang JF, Zhou Y, Yoon J, Kim Y, Kim SJ, Kim JS (2010) Naphthalimide modified rhodamine derivative: Ratiometric and selective fluorescent sensor for Cu^{2+} based on two different approaches. Org Lett 12:3852–3855
15. Kang H, Fan C, Xu H, Liu G, Pu S (2018) A highly selective fluorescence switch for Cu^{2+} and Fe^{3+} based on a new diarylethene with a triazole-linked rhodamine 6G unit. Tetrahedron 74:4390–4399
16. Qin JC, Yang ZY, Wang GQ, Li CR (2015) FRET-based rhodamine–coumarin conjugate as a Fe^{3+} selective ratiometric fluorescent sensor in aqueous media. Tetrahedron Lett 56:5024–5029
17. You Q-H, Huang H-B, Zhuang Z-X, Wang X-R, Chan W-H (2016) A new rhodamine-based fluorescent probe for the discrimination of Fe^{3+} from Fe^{2+}. Bull Kor Chem Soc 37:1772–1777
18. Ge F, Ye H, Zhang H, Zhao B-X (2013) A novel ratiometric probe based on rhodamine B and coumarin for selective recognition of Fe(III) in aqueous solution. Dyes Pigments 99:661–665
19. Zhao J, Gao Q, Zhang F, Sun W, Bai Y (2016) Two colorimetric fluorescent probes for detection Fe^{3+}: synthesis, characterization and theoretical calculations. J Lumin 180:278–286
20. Chen X, Sun W, Bai Y, Zhang F, Zhao J, Ding X (2018) Novel rhodamine Schiff base type naked-eye fluorescent probe for sensing Fe(3+) and the application in cell. Spectrochim Acta A Mol Biomol Spectrosc 191:566–572
21. Zhang J, Zhang L, Wei Y, Chao J, Shuang S, Cai Z, Dong C (2014) A selectively rhodamine-based colorimetric probe for detecting copper(II) ion. Spectrochim Acta A Mol Biomol Spectrosc 122:191–197
22. Hao Z, Fan J, Jing L, Hu M, Cao J, Jing W, Li H, Liu X, Peng X (2012) Optical Cu^{2+} probe bearing an 8-hydroxyquinoline subunit: high sensitivity and large fluorescence enhancement. Talanta 93:55
23. Bao X, Cao X, Nie X, Xu Y, Guo W, Zhou B, Zhang L, Liao H, Pang T (2015) A new selective fluorescent chemical sensor for Fe^{3+} based on rhodamine B and a 1,4,7,10-tetraoxa-13-azacyclopentadecane conjugate and its imaging in living cells. Sensors Actuators B Chem 208:54–66
24. Li Z, Zhao JL, Wu YT, Mu L, Zeng X, Jin Z, Wei G, Xie N, Redshaw C (2017) Highly selective recognition of Al(3+) and I(−) ions using a bi-functional fluorescent probe. Org Biomol Chem 15:8627–8633
25. Ruan Q, Mu L, Zeng X, Zhao JL, Zeng L, Chen ZM, Yang C, Wei G, Redshaw C (2018) A three-dimensional (time, wavelength and intensity) functioning fluorescent probe for the selective recognition/discrimination of cu(2+), hg(2+), Fe(3+) and F(−) ions. Dalton Trans 47:3674–3678
26. Li X, Yin Y, Deng J, Zhong H, Tang J, Chen Z, Yang L, Ma LJ (2016) A solvent-dependent fluorescent detection method for Fe(3+) and hg(2+) based on a rhodamine B derivative. Talanta 154:329–334
27. OuYang H, Gao Y, Yuan Y (2013) A highly selective rhodamine-based optical–electrochemical multichannel chemosensor for Fe^{3+}. Tetrahedron Lett 54:2964–2966 26
28. Chai M, Zhang D, Wang M, Hong H, Ye Y, Zhao Y (2012) Four rhodamine B-based fluorescent chemosensor for Fe^{3+} in aqueous solution. Sensors Actuators B Chem 174:231–236
29. Liu Y, Shen R, Ru J, Yao X, Yang Y, Liu H, Tang X, Bai D, Zhang G, Liu W (2016) A reversible rhodamine 6G-based fluorescence turn-on probe for Fe^{3+} in water and its application in living cell imaging. RSC Adv 6:111754–111759
30. Kagit R, Yildirim M, Ozay O, Yesilot S, Ozay H (2014) Phosphazene based multicentered naked-eye fluorescent sensor with high selectivity for Fe^{3+} ions. Inorg Chem 53:2144–2151
31. Yan L, Yang M, Leng X, Zhang M, Long Y, Yang B (2016) A new dual-function fluorescent probe of Fe^{3+} for bioimaging and probe-Fe^{3+} complex for selective detection of CN^-. Tetrahedron 72:4361–4367

32. Senthil Murugan A, Vidhyalakshmi N, Ramesh U, Annaraj J (2018) In vivo bio-imaging studies of highly selective, sensitive rhodamine based fluorescent chemosensor for the detection of Cu^{2+}/Fe^{3+} ions. Sensors Actuators B Chem 274:22–29
33. Wang Y, Song F, Zhu J, Zhang Y, Du L, Kan C (2018) Highly selective fluorescent probe based on a rhodamine B and furan-2-carbonyl chloride conjugate for detection of Fe^{3+} in cells. Tetrahedron Lett 59:3756–3762
34. Sharma N, Reja SI, Gupta N, Bhalla V, Kaur D, Arora S, Kumar M (2017) A highly selective fluorescent probe for Fe^{3+} in living cells: a stress induced cell based model study. Org Biomol Chem 15: 1006–1012
35. Weerasinghe AJ, Schmiesing C, Varaganti S, Ramakrishna G, Sinn E (2010) Single- and multiphoton turn-on fluorescent Fe^{3+} sensors based on Bis(rhodamine). J Phys Chem B 114:9413–9419
36. Liu P, Luo A, Wang Y, Hu J, Huang Q, Wang H (2018) A bis-(rhodamine)-based off–on colorimetric and fluorescent probe for Fe^{3+} ion detection in serum and bioimaging. Chem Pap 72:2575–2587
37. Zhao N, Xuan S, Fronczek FR, Smith KM, Vicente MGH (2017) Enhanced Hypsochromic shifts, quantum yield, and π–π interactions in a meso,β-Heteroaryl-fused BODIPY. J Organomet Chem 82:3880–3885
38. Kaewtong C, Noiseephum J, Uppa Y, Morakot N, Morakot N, Wanno B, Tuntulani T, Pulpoka B (2010) A reversible Em-FRET rhodamine-based chemosensor for carboxylate anions using a ditopic receptor strategy. New J Chem 34:1104–1108
39. Thordarson P (2011) Determining association constants from titration experiments in supramolecular chemistry. Chem Soc Rev 40: 1305–1323
40. Reed AE, Curtiss LA, Weinhold F (1988) Intermolecular interactions from a natural bond orbital, donor-acceptor viewpoint. Chem Rev 88:899–926
41. Pandith A, Kumar A, Kim HS (2015) 9-N-Alkylaminomethylanthracene probes for selective fluorescence sensing of pentafluorophenol. RSC Adv 5:81808–81816
42. Zhang Q, Liu X-J, He R-C, Guo C-B, Zhao W-Z, Zeng C-C, Yin L-P (2018) Development of a fluorescent-type sensor based on rhodamine B for Fe(III) determination. Chem Lett 47:122–125
43. Zhou T, Chen X, Hua Q, Lei W, Hao Q, Zhou B, Su C, Bao X (2017) Synthesis and evaluation of a new furfuran-based rhodamine B fluorescent chemosensor for selective detection of Fe^{3+} and its application in living-cell imaging. Sensors Actuators B Chem 253: 292–301
44. Mallick D, Biswal B, Thirunavoukkarasu M, Mohanty R, Bag B (2017) Signalling probes appended with two rhodamine derivatives: inter-component preferences, Fe(III)-ion selective fluorescence responses and bio-imaging in plant species. New J Chem 41:15144–15156